

Late Pleistocene-Holocene earthquake-induced slumps and soft-sediment deformation structures in the Acequion River valley, Central Precordillera, Argentina

Laura P. Perucca^{1,2,*}, Enrique Godoy³, Ana Pantano^{1,2}

¹ Consejo Nacional de Investigaciones Científicas y Técnicas (CONICET)

² Gabinete de Neotectónica. INGENIO. Facultad de Ciencias Exactas, Físicas y Naturales. Universidad Nacional de San Juan, Av. Ignacio de La Roza y Meglioli s/n (5400), San Juan, Argentina; e-mail: lperucca@unsj-cuim.edu.ar; anapantano7@gmail.com

³ Departamento Geología, Facultad de Ciencias Exactas, Físicas y Naturales, Universidad Nacional de San Juan, Av. Ignacio de La Roza y Meglioli s/n (5400), San Juan, Argentina; e-mail: quiquecalcite@gmail.com

* Corresponding author

Abstract

Evidence of earthquake-induced liquefaction features in the Acequión river valley, central western Argentina, is analysed. Well-preserved soft-sediment deformation structures are present in Late Pleistocene deposits; they include two large slumps and several sand dikes, convolutions, pseudonodules, faults, dish structures and diapirs in the basal part of a shallow-lacustrine succession in the El Acequión River area. The water-saturated state of these sediments favoured deformation.

All structures were studied in a natural trench created as a result of erosion by a tributary of the Acequión River, called El Mono Creek. They form part of a large-scale slump system. Two slumps occur in the western portion of the trench and must have moved towards the ENE (70°), where the depocentre of the Boca del Acequión area is situated. Considering the spatial relationship with Quaternary faults, the slumps are interpreted as being due to a seismic event. The thickest dikes in the El Mono Creek trench occur in the eastern portion of the trench, indicating that the responsible earthquake was located to the east of the study area, probably at the Cerro Salinas fault system zone.

The slumps, sand dikes and other soft-sediment deformation features are interpreted as having been triggered by earthquakes, thus providing a preliminary palaeoseismic record of the Cerro Salinas fault system and extending the record of moderate- to high-magnitude earthquakes in central western Argentina to the Late Pleistocene.

Keywords: lacustrine sedimentation, liquefaction, seismites, slumps, soft-sediment deformation structures, palaeo-earthquakes

1. Introduction

Central western Argentina, including the study area situated in the border zone between the provinces of San Juan and Mendoza, has been affected by at least nine destructive earthquakes ($M_s \geq 6.3$) during the last 300 years. These earthquakes caused

severe damages and secondary effects, such as landslides and liquefaction phenomena (Perucca & Moreiras, 2006).

The Acequión river valley is located 120 km south of San Juan City (San Juan province) at 32°15' S and 68°45' W (Fig. 1A). The Acequión River is a permanent stream that runs to the SE through the

Cambro-Ordovician calcareous rocks of the Sierra de Pedernal-Los Pozos. Some evidence of Quaternary faulting between two structural systems was found recently; the activity appears characterised by reverse faults with regionally an N-S strike and an opposite vergence. The faults occur in this valley between Cordón de Santa Clara and the Sierra de Pedernal-Los Pozos (Perucca et al., 2012) (Fig. 1B,C).

Two rock avalanches located south of the Sierra de Pedernal have dammed the Acequión River, which resulted in the development of lakes (Perucca et al., 2009) that were radiocarbon dated as formed between 7497 ± 157 age BP and 32680 ± 1580 BP (Perucca et al., 2009, 2012).

The lacustrine succession is built by brownish fine-grained sediments with intercalations of sandy

clay. The layers are poorly consolidated, well sorted, and thin to intermediate in thickness, with a total thickness of 10 m. The sandy layers are thicker at the western side of the area, whilst interbedded clay, silt and thin sand layers predominate towards the east. The deformed deposits of the Late Pleistocene lake (cf. Tian et al., 2014, this issue) are covered by Holocene fan conglomerates (gravels) which could be correlated all over the study area.

Here we describe several of the soft-sediment deformation features, faults and two slumps located in a natural trench in the El Mono Creek. The deformation structures occur close to two active Holocene fault systems located nearby, viz. the Los Colorados-Acequión Thrust (3 km to the west) and the Precordillera Oriental-Cerro Salinas Fault system (18 km to the east) (Fig. 1B,C).

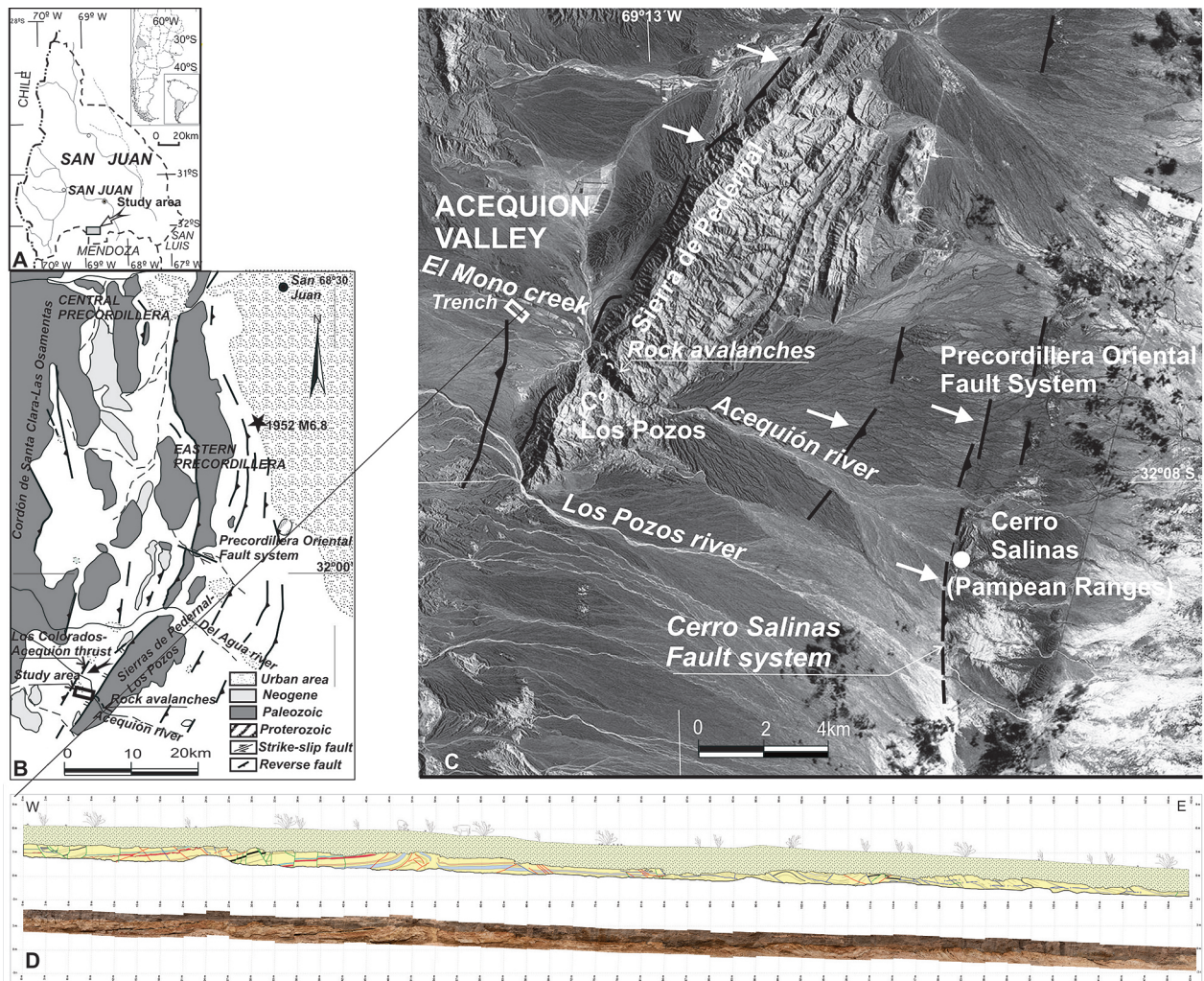


Fig. 1. Setting of the study area and of the investigated trench.

A: location of San Juan province in Argentina and South America; **B:** Schematic setting of the region with the epicentre of the 1952 earthquake; **C:** Satellite image (Google Earth) of the study area. White arrows point at the main Quaternary fault systems; **D:** Faults and slump features in the logged trench (150 m in the El Mono Creek).

2. Geological and tectonic setting

The active seismicity of the Andean back-arc in central western Argentina is related to the Pampean flat-slab segment of the Nazca Plate (between 28° S and 33° S), the activity of which started 8–10 Ma ago (Kay et al., 1991). In this area, Late Miocene-Quaternary tectonics has resulted in the development of the Principal and Frontal Cordilleras, Precordillera and the Pampean Ranges in the eastward foreland region (Ramos, 1988). This convergence between the Nazca and South America Plates resulted in a thin-skinned fold and thrust belt in the Central Precordillera and a thick-skinned tectonic style in the Eastern Precordillera and Pampean Ranges (Smalley et al., 1993).

This region is characterised by an intense shallow (5–50 km) seismic activity (Smalley & Isacks, 1990), but a moderate to high activity also exists between 90 and 150 km. At least nine destructive earthquakes occurred in the area in the past century and a half, viz. in 1861 (Ms 7.0), 1894 (Ms 7.5), 1903 (Ms 6.3), 1917 (Ms 6.5), 1920 (Ms 6.8), 1927 (Ms 7.1), 1952 (Ms 6.8), 1944 (Ms 7.4) and 1977 (Ms 7.4).

Quaternary deformation in the study area is mainly expressed by NNE-trending west-verging thrusts belonging to the Eastern Precordillera. The faults stretching for approx. 150 km along a N-S trend in the eastern flank of the Sierra de Pederal-Los Pozos is known as the Precordillera Oriental Fault system, an eastwards dipping reverse-fault system composed of several high-angle fault segments (see Fig. 1B,C) (see also Van Loon, 2014b, this issue). Recent activity of this fault system was related to the Ms 6.8 earthquake of June 10th, 1952 (Fig. 1B). After this earthquake, several secondary effects like fissures, liquefaction phenomena, and landslides were identified in areas nearby the epicentre. According to Perucca et al. (2009), the active Cerro Salinas Fault system, located 18 km east of the study area, is the most likely source area, for at least three earthquakes in the area (Fig. 1C). This fault system, belonging to the Precordillera Oriental Fault system, is an active fault zone with several reverse-fault segments affecting the western flank of a Quaternary anticline (Fig. 1B,C).

Furthermore, west of the area under study NNW-trending east-verging active thrusts prevail, related to the Central Precordillera (Los Colorados-Acequión Thrust) (Fig. 1B,C).

3. Methods

The palaeoseismicity of the Acequión River valley can be analysed through the earthquake-in-

duced effects preserved in the geological record and by applying empirical relationships based on the extension of surface ruptures or displacements (Obermeier et al., 2001). Extensive surveys were carried out along the outcrops of the palaeolake in order to locate deformation structures. A natural trench of 2 km long, trending WNW-ESE and created as a result of erosion by the Acequión River and now located in the El Mono Creek (a branch of the main stream) was used for study of the sedimentological structures; these were sketched, measured and photographed in the field (Fig. 1C,D). The lithology of both the deformed and the undeformed beds was described and samples of them were collected; moreover, a stratigraphic column repre-

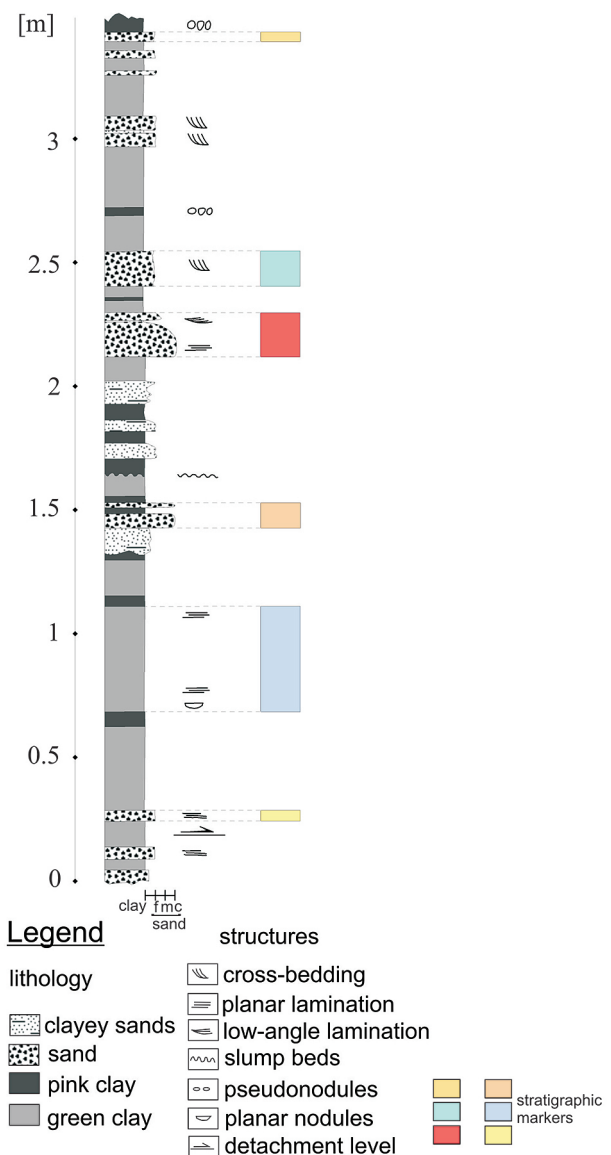


Fig. 2. Sedimentary log of the lacustrine succession in the El Mono Creek.

sentative of the section was drafted (Fig. 2). Many soft-sediment deformation features, among which sand dikes (see also Sarkar et al., 2014, this issue), convolutions, pseudonodules (see also Van Loon & Pisarska-Jamrozý, 2014), and dish structures (see

also He et al., 2014, this issue) were analysed, and their distribution was determined (Fig. 3).

For the study of the slumps in the trench, a 150-m long photo mosaic was prepared after a grid had been established in the outcrop (Figs. 1D, 4).

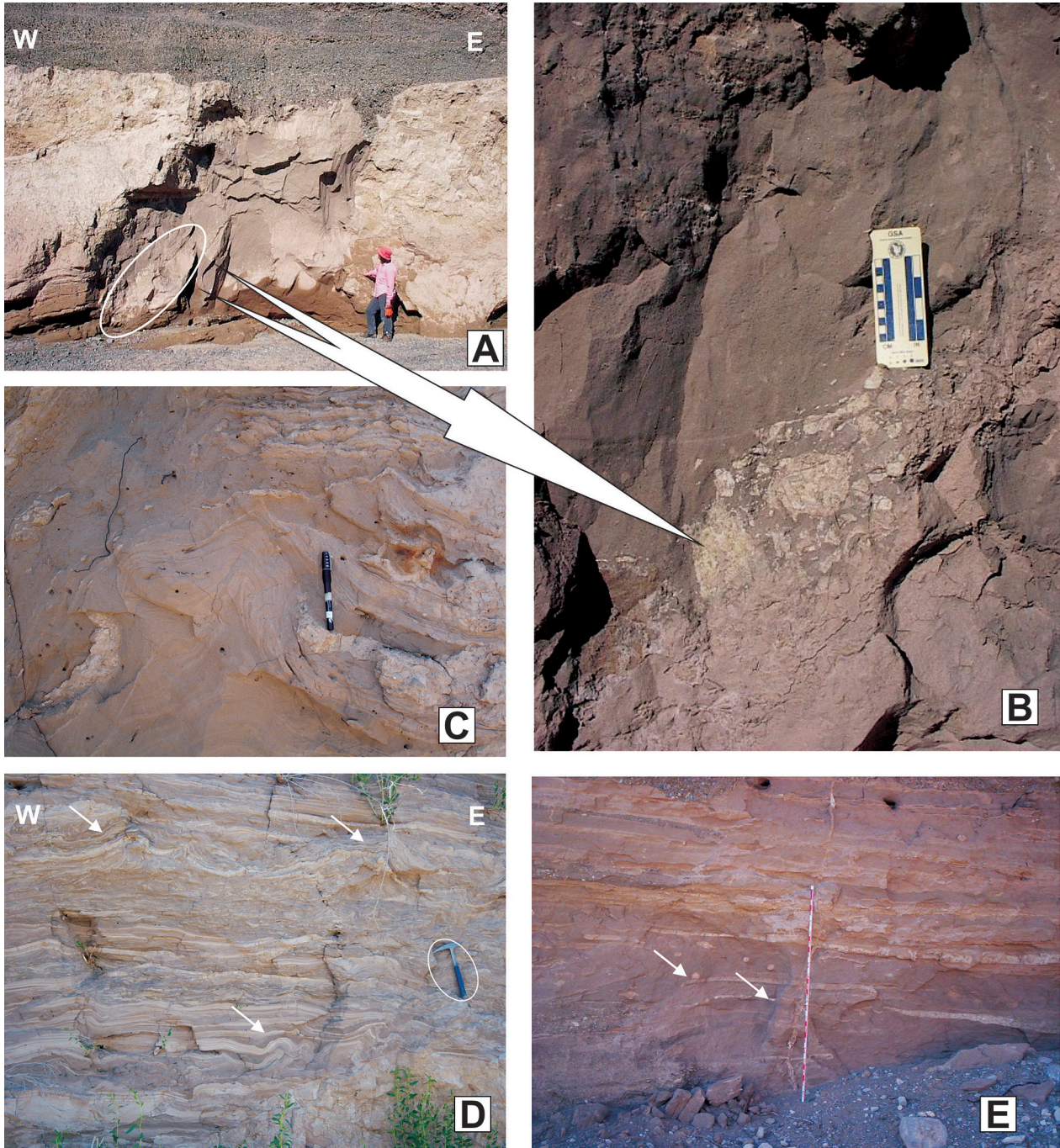


Fig. 3. Soft-sediment deformation features in the El Mono Creek.

A: Thick sand dike in the eastern part. The upper level of gravel is also disturbed. The fluidised sand layer shows flow structures indicating upward injection of the sand-filled clastic dike; **B:** Detail of the thick sand dike containing clasts of sidewall material (silt-clay); **C:** Sand diapir; **D:** Diapiric intrusion of clayey silt deforming the strata into recumbent folds; **E:** Clayey pseudonodules and dish structures.

The mosaic was used as a base for mapping in the trench, where structures were measured in detail to correlate individual layers and to define stratigraphic marker horizons; a schematic interpretation illustrating a classic slump profile and its evolution could thus be made (Fig. 5).

The results of the studies of the sediments in the trench were compared with previous studies in the area, but also with similar studies elsewhere (e.g. Seilacher, 1969, 1984; Tuttle & Seeber, 1991; Perucca et al., 2009).

4. Soft-sediment deformation features and slumps

In the eastern portion of the El Mono Creek (the natural trench which is exposed over a length of more than 250 m), sand dikes (see also Valente et al., 2014, this issue), diapirs, pseudonodules, dish structures and convolutions are the main soft-sediment deformation structures (Fig. 3). In the western part, two slumps are present; they have a total length of 120 m and are 2 m thick (Fig. 4). The slumping must have taken place in an ENE direction and the sediments involved must have been fresh and saturated with water.

4.1. Soft-sediment deformation structures

Sand dikes and diapirs occur at several levels of the Pleistocene sedimentary succession in the El Mono Creek (Fig. 3A). Dikes made up of large sand intrusions linked with small ones frequently form networks. The upward motion of sand is supported by the facts that major dikes derive from a basal sand bed and that contiguous layers show upward bending along the intrusions.

The sand dikes have in general an irregular form; they are 1–4 m thick and up to 4 m high. Figure 3(A,B) shows one of the larger sand dikes, in which a 3.6-m-wide feeder channel and areas of accumulation of angular clasts consisting of sidewall material (silty clay) are visible. The clasts are oriented in an upward direction, parallel to the boundary (Fig. 3B). Towards the top of the structure, a cap composed of gravel and sand is visible, accompanied by faults and smaller sand dikes with similar characteristics. The sand injections look like diapiric domes, sometimes rounded sometimes conical (Fig. 3C). The sand is not very cohesive, with mid-size ($1/4$ – $1/2$ mm), well sorted grains. No internal structures are visible and the contacts with the sidewall are mostly irregular.

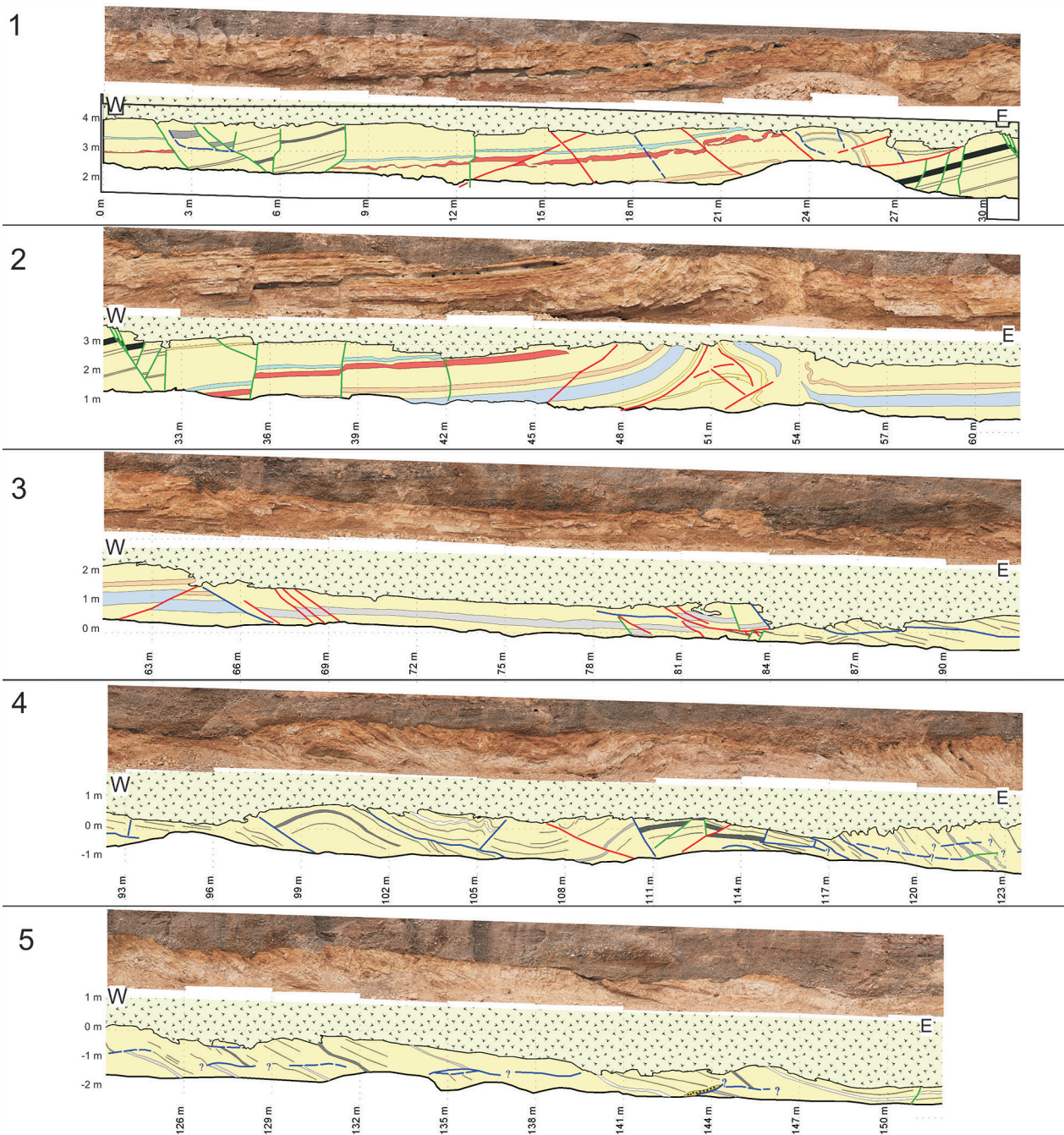
The thickest dikes (up to 4 m) are located in the eastern portion of the El Mono Creek; the width of the dikes decreases toward the west, where the sand dikes become eventually even less than 0.1 m wide.

Other structures that are due to liquefaction, such as water-escape structures, faulting (small scale) associated with folding, recumbent folds, ball-and-pillow structures, pseudonodules and convolute bedding are present east of the trench (Fig. 3D,E). These structures are restricted to single stratigraphic layers separated by undeformed beds and can be correlated over tens of metres.

Several lacustrine levels show disrupted lamination and kinds of convolute bedding forming recumbent or isoclinal folds along the El Mono Creek (see also Üner, 2014, this issue). Diapiric intrusion of clayey silt deformed the strata into flame-like recumbent folds with preservation of the primary stratification (Fig. 3D). The wavelengths of the folds vary from 30 to 100 cm and their amplitude is of the order of 10–15 cm; the characteristics of these recumbent folds are consistent with gravity collapse during shaking.



The upper contacts of these layers with the overlying strata are nearly flat, indicating that it was an internal flow within the sand layers that caused the convolutions. McKee et al. (1962) concluded that the dominant mechanism for the development of intraformational recumbent folding involves the drag of a flowing sediment-rich fluid mass of clayey silt material over water-saturated sand. We suggest that, in the El Mono Creek, the silty clay was deformed as a result of the combined effects of liquefaction and shear stress, generated by the passage of seismic waves. Towards the top of the succession, dish structures occur together with irregular, rounded clayey pseudonodules floating in a sand matrix (Fig. 3E).

The above structures were previously briefly described by Perucca et al. (2009). The main reason to pay some attention to them here, too, is that their setting and characteristics are of interest for the explanation of the genesis of the two large slumps that can be reconstructed on the basis of the data in the trench of the El Mono Creek. On the basis of their characteristics, Perucca et al. (2009) associated them with seismic events, also taking into consideration that they conform to the criteria laid down by Sims (1975): (1) they occur in a seismically active region of the Precordillera Oriental Fault system; (2) they are restricted to single layers separated by undeformed beds; (3) the structures are correlatable over a large area; (4) the layers are flat-lying, eliminating the influence of slope failure; (5) the structures are similar








Legend

lithology

-  post-deformational fanglomerates
-  deformed lacustrine deposits

structures

-  fracture
-  normal fault
-  reverse fault

-  bedding
-  sand dikes

-  stratigraphic markers
-  stratigraphic markers
-  stratigraphic markers
-  stratigraphic markers

Fig. 4. Field photographs and schematic interpretations of a metre-scale fold and thrust system related to the downslope (eastwards) movement. The ~150-m long trench comprises normal and strike-slip faults, thrusts and folds that developed below an undeformed succession of Pleistocene-Holocene fanglomerates.

to those described by several authors (Obermeier, 1994, 1998); and (6) there is evidence of liquefaction in all the large historical earthquakes that occurred in the region since the 1860s.

Although the above criteria have been discussed by numerous authors, they are now commonly considered as useful in practice (Van Loon, 2014a, this issue), although their application requires a critical consideration of the precise setting (Moretti & Van Loon, 2014)

4.2. Slump structures

West of the El Mono Creek, two slump structures occur that we interpret as related to a seismic event. Despite the uncertain origin of the slumps, their large size (up to 60 m long) and their close relationship with sand dikes and other seismically-induced structures strongly suggests that they were triggered by high-energy seismic events (Fig. 1D, 4). Slumps are very frequent in both subaqueous and subaerial lacustrine environments. Numerous examples have been studied in the field (e.g. Gibert et al., 2005), in cores (e.g. Bertrand et al., 2008) and through seismic profiling (e.g. Niemi & Ben-Avraham, 1994). It is obvious from all studies that two types of slump exist: (1) the most common type exists of masses that flow down over a sedimentary surface after liquefaction, commonly with a rotational component, and commonly with partial loss of inter-grain contacts (such slumps can easily pass into mudflows), and (2) masses that keep more or less their original shape and internal structure, but that slide a bit down, leaving a concave space in the underlying sediment and producing a 'high' at the sedimentary surface at their downward end. During this sliding, compression tends to occur on the toe and extension in the head area of the slump (Fig. 5A). It is this second type of slumping that took place in the area of the El Mono Creek.

The extensional areas of the slumps in the El Mono Creek show several features like listric and/or normal faults and rollover anticlines (Fig. 5), which were generated in the head zone of the slumps (cf. Lewis, 1971). The compressional features related with the slump movement are, in contrast, located in the east. These structures are thrusts, duplexes, downslope-vergent (to the east) folds generated on the toe part of the slump (Fig. 5). There, its movement is being stopped, probably due to a decreasing inclination of the slope (cf. Lewis, 1971). The layers between the tensional and compressional zones do not show deformation (Fig. 5).

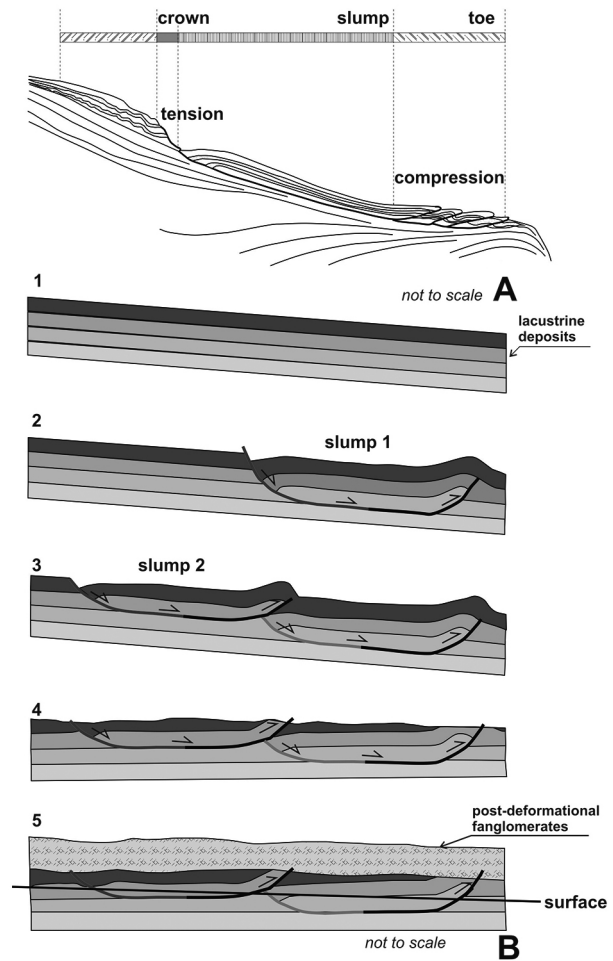


Fig. 5. Schematic model of the slump development (not to scale). **A**: classic slump profile (from Lewis, 1971); **B**: evolution of the two slumps (modified from Alsop & Marco, 2013).

5. Discussion

Soft-sediment deformation in lacustrine sediments can take place due to liquefaction resulting from pore-pressure changes associated with rapid fluctuations in the lake level, from inherent sediment instability and from earthquake-triggered shocks. In the deformed zones in the El Mono Creek exposure, the facies changes laterally; however, the deformation is consistent with different styles and can be seen in a range of sedimentological settings. This eliminates the possibility that the deformation in the El Mono Creek resulted exclusively from intrinsic instabilities in the sediments. The styles of deformation (as seen in the Acequión river area) in the above-mentioned sedimentary environment are not easy to explain by pore-pressure changes temporarily induced by a rapid fall or rise of the water level. Taking also into account the frequent

occurrence of moderate-to high-magnitude earthquakes in the area, the deformations can therefore be explained satisfactorily only as a result of earthquake-induced liquefaction. This led to sediment layers of different density breaking up and penetrating (downwards or upwards) adjacent layers forming typical flow and injection structures.

The study of seismites is very important for the reconstruction of the palaeoseismic history of a region; such a study can be carried out by determining the seismic nature of the various seismogenic features, as well as by establishing the magnitude and date of the earthquake (Michetti et al., 2005). Most intense and abundant soft-sediment deformation features are related to a nearby seismic area, as indicated by the spatial distribution of sand dikes and the size of associated structures. Besides, the magnitudes of palaeo-earthquakes can be estimated in other areas by noting the regional extent and size of liquefaction features and comparing these data to similar features resulting from known earthquakes in similar settings (Munson et al., 1995; Obermeier, 1994, 1998). Seismically induced pseudonodules require earthquake magnitudes probably exceeding a magnitude of 6.5 for their formation; sand dikes and pillow structures have been interpreted as related to earthquakes of magnitudes ranging from 5 to 8 (Obermeier et al., 2001). Owen & Moretti (2011) pointed out, however, that also other factors influence the size, so that the sizes of soft-sediment deformations may not be an adequate indicator of earthquake magnitude.

Even though several autogenic trigger mechanisms that are directly associated with sedimentation processes and patterns can generate slumps in lakes, such as oversteepening or sedimentary overloading (Lewis, 1971; Allen, 1982; Owen & Moretti, 2011), many slumps have been attributed to allogenic trigger mechanisms, such as earthquakes (García-Tortosa et al., 2011). There are numerous examples in the geological record (Karlin et al., 2004) related to historical earthquakes (Schnellmann et al., 2002) and even modern earthquakes (Niemi & Ben-Avraham, 1994). It is now well known that many examples of slumps may be attributed to earthquakes in central-western Argentina. Soft-sediment deformation features and many slumps are generated by earthquake-induced shocks (Allen, 1975; Youd, 1978, 1986; Seed et al., 1983; Schnellmann et al., 2002). Atkinson (1984) mentioned that an earthquake of magnitude 5 can induce liquefaction when suitable conditions exist; Keefer (1987) established a magnitude >5.0 for subaqueous slumps.

It is worth mentioning in this context that studies of modern sediments show that slumps and

slides can occur on very gentle slopes (0.25°) (Field et al., 1982; García-Tortosa et al., 2011; Van Loon et al., 2012; Su & Van Loon, 2014), which is not yet generally recognised.

Perucca et al. (2009) mentioned that liquefaction phenomena, as well as many landslides, were generated during all earthquakes with $M_s \geq 6.3$ that occurred during the 19th and 20th centuries in the provinces of San Juan and Mendoza. Furthermore, liquefaction structures occur in the water-saturated Holocene dammed-lake succession in an extensive area. Although slumps are not structures that are diagnostic for seismic activity, their abundance and proximity to the probable epicentres may point at tectonic instability of the area. Moreover, these structures are also associated with sand dikes, soft-sediment deformation features and faults, which supports our interpretation.

From the observations and measurements made in the slumps and the detailed analysis of the profile in the El Mono Creek, it must be deduced that in the western area normal faults alternate with reverse faults the azimuths of which coincide with the azimuths of the strata (320° – 340°). A subhorizontal, thick detachment bed was displaced nearly 150 m towards the East. The various parts of the two slumps are exposed in the El Mono Creek, with extensional structures in the head zone and contractional features in the intermediate and toe zones.

More to the east in the El Mono creek, the widths and quantity of sand dikes increase; domes, dish structures, joints, and sand-filled fissures also increase in size towards the East. Soft-sediment deformation features were not found in the western sector of this palaeolake, nor in northern and southern gullies that were eroded into these deposits.

As mentioned above, the thickest 4-m-wide sand dikes and the main soft-sediment deformation structures are exposed in the eastern part of the lacustrine deposits. The width of the sand dikes decreases towards the west, suggesting (cf. Tuttle, 2001) that the epicentre was situated east of the study area (Perucca et al., 2009).

Perucca et al. (2009) estimated the magnitude of the earthquake on the basis of the distance (d) to the energy centre (Obermeier & Pond, 1999; Obermeier et al., 2001). They assumed that the soft-sediment deformation features in the Acequión area were formed during Late Pleistocene-Holocene activity of the Cerro Salinas Fault system; the minimum magnitude of the triggering earthquake was estimated as $M > 6.3$ – 6.7 considering the maximum distance ($d = 18$ km) between seismites and the nearest possible epicentre (Cerro Salinas Fault system).

6. Conclusions

A variety of soft-sediment deformation structures, including folds, ball-and-pillow structures, pseudonodules, faults, load casts, sand-filled dikes and slumps developed during sedimentation in a Late Pleistocene shallow-lacustrine environment. They occur in the vicinity of the active Cerro Salinas Fault system. These soft-sediment deformation structures in the El Acequión River area are interpreted as having been caused by earthquake-related shocks, because of their similarity to other structures that are known to have been caused by historical earthquake-induced structures in the region, and also due to the distribution and lateral extent of the deformations. The soft-sediment deformation structures were among the most widespread and spectacular results of the historical seismic shocks. They have been described from all earthquakes with $M > 6.3$ that occurred during the 19th and 20th centuries in the provinces of San Juan and Mendoza (Perucca & Moreiras, 2006).

Moreover, the Quaternary Cerro Salinas Fault system, a N-S trending fault located 18 km east of the study area, is suggested as the epicentre of these earthquakes ($M > 5.5$ and distance to the epicentre less than 25 km) in accordance with the characteristics and distribution of the soft-sediment deformation structures.

Understanding of the evolution of the seismites and slumps and of the underlying physics is key factor for a reliable reconstructing of the characteristics and number of ancient earthquakes. The deformations described and interpreted here may help to deepen this understanding. They are thus also useful tools to understand the behaviour of the areas susceptible to soft-sediment deformation during future earthquakes, which can help to mitigate damage and to save lives.

Acknowledgements

The authors especially thank the reviewers for their helpful comments. Special thanks to N. Vargas, for his helpful assistance during fieldwork. Finally, the authors acknowledge funding received from PID 0799 of the Consejo Nacional de Investigaciones Científicas y Técnicas (CONICET), PICTO 2009-UNSJ-0013 and CICITCA 21E870 to support this research.

References

Allen, J., 1975. Geologic criteria for evaluating seismicity. *Geological Society of America Bulletin* 86, 1041–1056.

- Allen, J., 1982. Sedimentary structures, their character and physical basis. *Developments in Sedimentology* 2, 663 pp.
- Alsop, I. & Marco, S., 2013. Seismogenic slump folds formed by gravity-driven tectonics down a negligible subaqueous slope. *Tectonophysics* 605, 48–69.
- Atkinson, G., 1984. Simple computation of liquefaction probability for seismic hazard applications. *Earthquake Spectra* 1, 107–123.
- Bertrand, S. Charlet, F., Chapron, E., Fagel, N. & De Baptist, M., 2008. Reconstruction of the Holocene seismotectonic activity of the Southern Andes from seismites recorded in Lago Icalma, Chile, 39°S. *Palaeogeography Palaeoclimatology Palaeoecology* 259, 301–322.
- Field, M.E., Gardner, J.V., Jennings, A.E. & Edwards, B.D., 1982. Earthquake-induced sediment failures on a 0.25° slope, Klamath River delta, California. *Geology* 10, 542–546.
- García-Tortosa, F.J., Alfaro, P., Gibert, L. & Scott, G., 2011. Seismically induced slump on an extremely gentle slope (<1°) of the Pleistocene Tecopa paleolake (California). *Geology* 39, 1055–1058.
- Gibert, L., Sanz de Galdeano, C., Alfaro, P., Scott, G. & Lopez Garrido, A.C., 2005. Seismic induced slump in Early Pleistocene deltaic deposits of the Baza Basin (SE Spain). *Sedimentary Geology* 179, 279–294.
- He, B., Qiao, X., Jiao, C., Xu, Z., Cai, Z., Guo, X., Zhang, Y. & Zhang, M., 2014. Paleo-earthquake events in the late Early Palaeozoic of the central Tarim Basin: evidence from deep drilling cores. *Geologos* 20, 105–123.
- Karlin, R.E., Holmes, M., Abella, S. & Sylwester, R., 2004. Holocene landslides and a 3500-year record of Pacific Northwest earthquakes from sediments in Lake Washington. *Geological Society of America Bulletin* 116, 94–108.
- Kay, S., Mpodozis, C., Ramos, V. & Munizaga, F., 1991. Magma source variations for mid-late Tertiary magmatic rock associated with a shallowing subduction zone and a thickening crust in the central Andes (28° to 33°S). [In:] R.S. Harmon & C. W. Rapela (Eds): Andean magmatism and its tectonic setting. *Geological Society of America Special Paper* 265, 113–137.
- Keefer, D.F., 1987. Landslides as indicators of prehistoric earthquakes. Directions in paleoseismology. *U.S. Geological Survey Open File report* 87–673, 178–180.
- Lewis, K.B., 1971. Slumping on a continental slope inclined at 1°–4°. *Sedimentology* 16, 97–110.
- McKee, E.D., Reynolds, M.A. & Baker, C.H., 1962. Experiments on intraformational recumbent folds in cross-bedded sand. *U.S. Geological Survey Professional Paper* 450-D, 155–160.
- Michetti, A.M., Audemard, F.A., & Marco S., 2005. Future trends in paleoseismology: integrated study of the seismic landscape as a vital tool in seismic hazard analyses. *Tectonophysics* 408, 3–21.
- Moretti, M. & Van Loon, A.J., 2014. Restrictions to the application of ‘diagnostic’ criteria for recognizing ancient seismites. *Journal of Palaeogeography* 3, 13–24.
- Munson, P., Munson, C. & Pond, E., 1995. Paleoliquefaction evidence for a strong Holocene earthquake in south-central Indiana. *Geology* 23, 325–328.

- Niemi, T.M. & Ben-Avraham, Z., 1994. Evidence for Jericho earthquakes from slumped sediments of the Jordan River delta in the Dead Sea. *Geology* 22, 395–398.
- Obermeier, S.F., 1994. Using liquefaction-induced features for paleoseismic analysis. [In:] S. Obermeier & W. Jibson (Eds): *Using ground-failure features for paleoseismic analysis*. U.S. Geological Survey Open-File Report 94, A1-A98.
- Obermeier, S.F., 1998. Liquefaction evidence for strong earthquakes of Holocene and latest Pleistocene ages in the states of Indiana and Illinois, USA. *Engineering Geology* 50, 227–254.
- Obermeier, S.F. & Pond, E.C., 1999. Issues in using liquefaction features for paleoseismic analysis. *Seismological Research Letters* 70, 34–58.
- Obermeier, S.F., Pond, E.C. & Olson, S.C., 2001. Paleoliquefaction studies in continental settings: geological and geotechnical features in interpretations and back analysis. *U.S. Geological Survey Open File Report* 01–29, 75 pp.
- Owen, G. & Moretti, M., 2011. Identifying triggers for liquefaction-induced soft-sediment deformation in sands. *Sedimentary Geology* 235, 141–147
- Perucca, L.P. & Moreiras, S.M., 2006. Liquefaction phenomena associated with historical earthquakes in San Juan and Mendoza provinces, Argentina. *Quaternary International* 158, 96–109.
- Perucca, L., Moreiras, S. & Bracco, A., 2009. Determination of seismogenic structures and earthquake magnitude from seismites in Holocene lacustrine deposits, Precordillera Range, central-western Argentina. *Journal of Iberian Geology*, 10–20.
- Perucca, L., Audemard, F.A., Pantano, A., Vargas, H.N., Avila, C.R. & Onorato, M.R., 2012. Vergencias opuestas cuaternarias en el área de Acequión, Precordillera de San Juan (Argentina). *Revista de la Sociedad Geológica de España* 25, 5–15.
- Ramos, V., 1988. The tectonics of the central Andes: 30° to 33° S latitude. [In:] S. Clark & D. Burchfield (Eds): *Processes in continental lithospheric deformation*. Geological Society of America Special Paper 218, 31–54.
- Sarkar, S., Choudhuri, A., Banerjee, S., Van Loon, A.J. & Bose, P.K., 2014. Seismic and non-seismic soft-sediment deformation structures in the Proterozoic Bhandar Limestone, central India. *Geologos* 20, 89–103.
- Seed, H., Idriss, I. & Arango, I., 1983. Evaluation of liquefaction potential using field performance data. *Journal of Geotechnical Engineering* 109, 458–482.
- Seilacher, A., 1969. Fault-graded beds interpreted as seismites. *Sedimentology* 13, 155–159.
- Seilacher, A., 1984. Sedimentary structures tentatively attributed to seismic events. *Marine Geology* 55, 1–12.
- Smalley, R.F. & Isacks, B.L., 1990. Seismotectonic of thin and thick-skinned deformation in the Andean foreland from local network data: evidence for a seismogenic lower crust. *Journal of Geophysical Research* 95, 12487–12498.
- Smalley Jr, R., Pujol, J., Regnier, M., Chiu, J., Chatelain, J., Isacks, B., Araujo, M. & Puebla, N., 1993. Basement seismicity beneath the Andean Precordillera thin-skinned thrust belt and implications for crustal and lithospheric behavior. *Tectonics* 12, 63–76.
- Schnellmann, M., Anselmetti, F.S., Giardini, D., McKenzie, J.A. & Ward, S.N., 2002. Prehistoric earthquake history revealed by lacustrine slump deposits. *Geology* 30, 1131–1134.
- Su, D., Van Loon, A.J., 2014. Sliding of a large block in an epeiric sea (Middle Cambrian Zhangxia Formation, SE Beijing, China). *Palaeogeography* 4 (in press).
- Tian, H.S., Zhang, B.H., Zhang, S.H. & Lü, M.Y., 2014. Neogene seismites and seismic volcanic rocks in the Linqiu area, Shandong Province, E China. *Geologos* 20, 125–137.
- Tuttle, M. & Seeber, L., 1991. Historic and prehistoric earthquake-induced liquefaction in Newbury, Massachusetts. *Geology* 19, 594–597.
- Tuttle, M., 2001. The use of liquefaction features in paleoseismology: lessons learned in the New Madrid seismic zone, central United States. *Journal of Seismology* 5, 361–380.
- Üner, S., 2014. Seismogenic structures in Quaternary lacustrine deposits of Lake Van (eastern Turkey). *Geologos* 20, 79–87.
- Valente, A., Ślącza, A. & Cavuoto, G., 2014. Soft-sediment deformation in Miocene deep-sea clastic deposits (Cilento, southern Italy). *Geologos* 20, 67–78.
- Van Loon, A.J., 2014a. The life cycle of seismite research. *Geologos* 20, 61–66.
- Van Loon, A.J., 2014b. The Mesoproterozoic ‘seismite’ at Laiyuan (Hebei Province, E China) re-interpreted. *Geologos* 20, 139–146.
- Van Loon, A.J. & Pisarska-Jamroży, M., 2014. Sedimentological evidence of Pleistocene earthquakes in NW Poland induced by glacio-isostatic rebound. *Sedimentary Geology* 300, 1–10.
- Van Loon, A.J., Han, Z. & Han, Y., 2012. Slide origin of breccia lenses in the Cambrian of the North China Platform: new insight into mass transport in an epeiric sea. *Geologos* 18, 223–235.
- Youd, T.L., 1978. Major cause of earthquake damage in ground failure. *Civil Engineering* 48, 47–51.

Manuscript submitted 31 October 2013

Revision accepted 14 December 2013